Title

HIGH RESOLUTION ELECTRON MICROSCOPY OF INTERFACES IN TOPOTAXIAL AND EPITAXIAL REACTIONS

Authors

Bahmen, U.
Douin, J.
Hetherington, C.J.D.

Publication Date

1988-12-01

LBL-26545

Lawrence Berkeley Laboratory
UNIVERSITY OF CALIFORNIA

Materials & Chemical Sciences Division

National Center for Electron Microscopy

Presented at the MRS Symposium on High Resolution Microscopy of Materials, Boston, MA, November 27–December 4, 1988

High Resolution Electron Microscopy of Interfaces in Topotaxial and Epitaxial Reactions

U. Dahmen, J. Douin, C.J.D. Hetherington, and K.H. Westma

December 1988

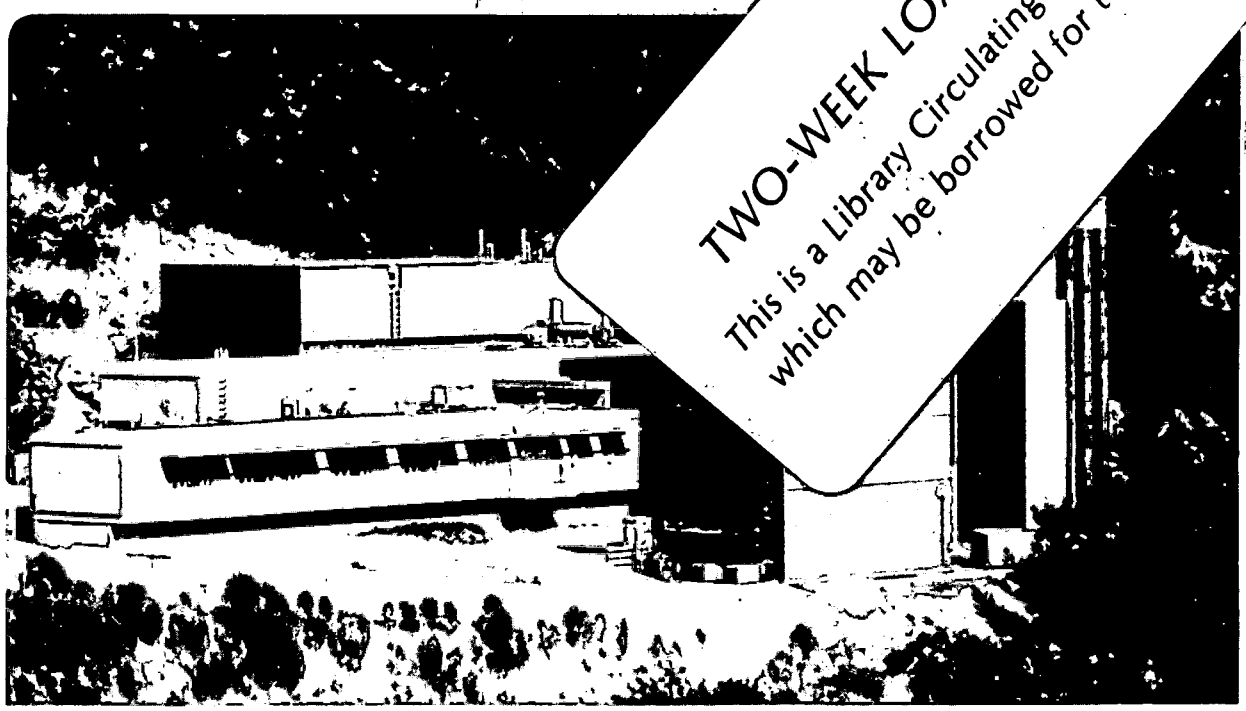

Prepared for the U.S. Department of Energy under Contract Number DE-AC03-76SF00098.

DISCLAIMER

HIGH RESOLUTION ELECTRON MICROSCOPY OF INTERFACES IN TOPOTAXIAL AND EPITAXIAL REACTIONS

U. DAHMEN, J. DOUIN, C.J.D. HETHERINGTON AND K.H. WESTMACOTT,
National Center for Electron Microscopy, Lawrence Berkeley Laboratory, University of California, Berkeley, CA 94720.

ABSTRACT

In the study of interfaces, HREM is most useful when the interface is viewed edge-on while both crystals are accurately aligned along low index zone axes. The formation of such interfaces by epitaxy or topotaxy is the natural means of obtaining structures that can be usefully analyzed by HREM. Furthermore, there is intense interest in understanding the atomic structure of such interfaces in a variety of technologically important materials. This contribution addresses such structures produced by thermal decomposition, precipitation reactions and ionized-cluster-beam deposition, and reports on the structural investigation of symmetrical and asymmetrical grain boundaries, precipitate/matrix interfaces, internal defect structure of precipitates and nanocrystalline composites.

INTRODUCTION

The optimum interface for characterization by high resolution electron microscopy (HREM) is one in which low index zone axes in the two crystals are parallel to each other and lie in the interface. Only for this special geometry is it possible to obtain simultaneously structure images of both crystals adjacent to the interface while the boundary itself is viewed edge-on. This imposes stringent conditions on the crystallography of such boundaries: 1) the orientation relationship between the two adjacent crystals must be special, and 2) the boundary, although it does not have to be planar, must lie in the zone of the parallel zone axes.

It might appear as though these conditions would severely limit the useful application of high resolution microscopy in the study of interfaces. However, because symmetrical geometries correspond to extrema in energy[1], special boundaries are favored over general boundaries. Due to their relative simplicity, symmetrical geometries are also preferred by theoreticians who model interface structure. It is thus fortunate that the specialized boundaries that can be characterized by high resolution microscopy are precisely the ones that allow the critical comparison between theory and experiment. This is particularly relevant for grain boundaries where modelling of atomic relaxations is presently limited to rational boundaries with distinct structural repeat units[2].

HREM is clearly most useful if the interface is edge-on, and most of the figures in this paper show edge-on boundaries. However, the potential of HREM for studying inclined or even face-on boundaries should not be overlooked[3]. Even if relaxations at the interface are obscured, rigid shifts (by a fraction of a unit cell) of the lattices across an inclined boundary can still be detected directly, through a change in the Moiré or the convergent beam diffraction pattern[4].

In the case of general heterophase interfaces between different crystal structures, especially in situations where strain energy dominates, irrational orientation relationships and high index boundary planes are commonplace[5]. In this case the application of high resolution microscopy is more complex and it is necessary to deduce the structure of the interface from high resolution images in several crystal orientations. Furthermore it is important to use all the information available from both high resolution and conventional analysis, including the diffraction contrast from strain fields.

In this contribution emphasis will be placed on epitaxial and topotaxial reactions in which symmetry is inherent in the reaction process. Such transformations are the most likely to provide the kind of interface that is preferred

by nature, the kind that can be characterized by HREM and the kind that can be handled by theory.

DECOMPOSITION REACTIONS

Topotaxial transformations are typified by solid-state reactions in which a parent phase transforms to a product phase with a well-defined orientation relationship[6]. An example is the thermal decomposition of $Mg(OH)_2$ to MgO and water vapor[7]. The orientation relationship between the parent hydroxide ($Mg(OH)_2$) phase and the product oxide (MgO) is one in which the threefold axes are aligned. Although the oxide is highly porous due to escape of the water vapor it maintains a surprisingly high degree of orientation. As a result, the product phase is an oriented collection of extremely small crystallites, or an example of a mosaic crystal[8]. Fig. 1 shows a high resolution micrograph of such a microstructure. The removal of the water vapor leaves behind a pore volume of ~55% and the structure may be regarded as a nanocomposite made up of roughly equal parts of pores and crystallites. The size and shape of the crystallites can be measured directly from micrographs such as the one shown in fig.1a. It is clear that even at this extremely small size (only a few unit cells) MgO crystals have strongly anisotropic shapes in which they are bounded by {100} planes. Edge lengths were found to vary in the range of roughly 0.8 to 3 nm and the particles often had unequal sides, i.e. they were orthorhombic, tetragonal and perhaps occasionally cubic in shape[9]. The three dimensional distribution of these nanocrystals determines the shape and distribution of the pores. Both stereomicroscopy and low angle electron diffraction techniques are presently being employed to determine the shape, size and spatial distribution of both pores and crystallites[10].

Most solid state thermal decomposition reactions of hydroxides and carbonates have similar characteristics to those of $Mg(OH)_2$, i.e. they are pseudomorphic and topotaxial with a large volume change that leads to a highly porous oriented aggregate of product phase. Another example of such a microstructure produced by thermal decomposition of $Al(OH)_3$ is seen in fig. 1b. By comparison with fig. 1a it is immediately apparent that the degree of orientation and the shape anisotropy of the nanocrystals is far less pronounced.

In order to study, by HREM, the development of interfacial structure during sintering, textured or oriented structures such as the ones illustrated here are clearly preferable to random grain structures which generally will not fulfill the special geometrical criteria outlined above.

PRECIPITATION REACTIONS

Precipitation reactions provide the most common examples of topotaxy. Most precipitates form in a well-defined orientation relationship with the matrix[5]. The orientation relationship also determines the minimum symmetry of the equilibrium shape of a particle[1]. At high aging temperature, precipitates tend to form in high symmetry morphologies while at low temperature and long aging times the same precipitates tend towards the minimum symmetry that is prescribed by the orientation relationship. This effect can be used in the HREM analysis of interfaces.

An example of θ' precipitates in an Al 4% Cu alloy heat treated in this manner is shown in fig. 2. θ' particles have bct crystal structure and form in a simple orientation relationship with the Al matrix in which a large number of common symmetry elements are maintained. The symmetry of the orientation relationship is tetragonal, the same as the point symmetry of the precipitate. The equilibrium particle shape must therefore have tetragonal or higher symmetry. This leads to the familiar circular plate morphology that forms at high aging temperature. However, faceted plates such as those shown in figure 2 can be produced by low temperature aging. This difference is equivalent to the roughening/faceting transition observed

at surfaces[11] which is an entropy effect and is likely to be of a general nature. Both morphologies are equally well

suited for high resolution microscopy of the broad interface of the plate. However, in order to obtain interpretable images of the plate edge, whose atomic structure is even more important in the growth process, only straight interfaces precisely parallel to the beam are suitable, and it is thus necessary to use the morphology obtained by low-temperature aging.

Figure 3 shows a high resolution image of such a plate. The edge of the plate is parallel to the beam and shows an interesting defect configuration. A dislocation, visible as an extra half plane, is attached to the very end of the particle. Close inspection shows that it is related to the presence of a dislocation loop in the θ'. Dislocations are frequently found associated with precipitates and are known to play an important role during the nucleation stage. It has been shown elsewhere that θ' precipitates can nucleate on existing dislocations that are dissociated by a reaction of the type 1/2 <110> →1/2 <100> + 1/2 <010> on a (100) plane[12]. As a result the interface at the plate edge can be viewed structurally as a stack of self-accommodating 1/2 <100> partial dislocations that change the atom plane stacking of the matrix to that of the precipitate. By growing faceted precipitates at low aging temperature it is thus possible to image the important atomic structure at both the edges and growth ledges.

A similar geometry has been obtained in an Al-Ag alloy where γ' $AgAl_2$ plates precipitate on {111} Al planes[13] and tend to form facets along <110> directions. A striking example of the structure at the end of a plate is seen in figure 4.

COMPARISON OF TOPOTAXIAL AND EPITAXIAL INTERFACE

During aging of Al-Si alloys, pure Si precipitates in almost pure Al in a rich variety of morphologies and orientation relationships[14]. The most noticeable particles are triangular plates on {111} planes with the Si and Al lattices in parallel (cube-cube) orientation[15]. The fact that the observed morphology of a plate is of lower than cubic symmetry has been related to the mechanism of growth which requires vacancies to accommodate the large volume increase on precipitation. The thickening of these plates occurs in discrete steps related to the existence of a near-coincidence site lattice in the cube-cube orientation relationship in which four spacings of the Al lattice correspond to three spacings of the Si lattice[16].

During the growth under three-dimensional constraint (solid state precipitation) the 3:4 coincidence of the two lattices is an important factor; however, it is uncertain whether this is also the case during growth under two-dimensional constraint (epitaxial growth). Vapor deposition of Al on {111} Si results in the same cube-cube orientation relationship observed for plate precipitates. A direct comparison of the same Al/Si heterophase interface grown by precipitation and ionized cluster beam deposition is thus of interest.

Fig. 5a shows a high resolution image of a Si plate precipitate in an Al matrix. The two crystals are viewed along their common <110> zone axis and thus the left edge as well as the broad faces of the precipitate are on edge while the right hand side of the particle is inclined and overlaps the matrix. This is consistent with the triangular shape of the plate known to be bounded by <110> directions. The most noticeable feature of the particle is its internally twinned structure. In fact only the central portion of the plate is in parallel, or cube-cube, orientation to the matrix while both the top and bottom broad interfaces are cube-twin related to the matrix. The same is apparently true for the short interface segments on the left edge of the plate. In the region of overlap between the central portion of the precipitate and the matrix a Moiré effect is clearly visible. Close inspection shows that this is due to the near 3:4 match between the two lattices. Note the apparent protrusions of Si on the broad interfaces, a feature unusual in well-defined planar interfaces as it is difficult to nucleate ledges on low-energy interfaces[17].

Image simulations of two alternative models of an unrelaxed interface are also shown in fig. 5. Fig. 5b is based on a model of the interface structure in which only

one Si bond is exposed to the Al and fig 5c is based on three Si bonds exposed to Al. By comparison of the image with the simulations it is clear that only the model in fig. 5b is correct.

A cross sectional view of an epitaxial interface produced by ionized cluster beam deposition, a low temperature technique known to promote the formation of high quality epitaxy, is shown in fig. 6. This interface is similar to the one formed by precipitation. However, note that the cube-twin relationship is not observed here. Instead, only parallel epitaxy is found. The interface is seen to be atomically flat with occasional ledges of single atomic height. The same interface produced by vapor deposition followed by annealing was investigated previously by HREM[18] and it was found that both possibilities exist, i.e. both single and triple Si bonds were coupled to the Al overlayer. These conclusions were confirmed here for ICB-grown Al by comparing the observed images with the two alternative simulated images.

SPECIAL GRAIN BOUNDARIES

Symmetry principles can also be applied to the formation of grain boundaries. It has recently been shown that a "continuous bicrystal" of Al can be produced by epitaxial thin film growth on a single crystal Si {100} surface, using the ionized cluster beam deposition technique[19,20]. Two grain orientations grow at 90° to one another, separated by continuously curved grain boundaries[21]. The morphology is similar to that of antiphase domains in ordered alloys. Typical bicrystal structures are illustrated in Figure 7. As-grown bicrystals tend to have random boundary orientations (figure 7a) while annealing at ~400°C produces highly faceted boundaries (figure 7b) It is clear that the more symmetrical boundaries lend themselves more easily to high resolution analysis and structural modeling.

Examples of the two types of facet characteristic for this 90°<110> misorientation are shown in figures 8 and 9. The symmetrical boundary in Figure 8 shows clear structural units in a relaxed periodic boundary while the asymmetrical boundary shown in Figure 9 does not reveal a clear periodicity, although atomic relaxations are quite apparent. In agreement with current models of grain boundary structure, the asymmetrical configuration in which low index planes are parallel to the boundary is clearly preferred over the symmetrical one. Image analysis and direct comparisons with proposed $\Sigma 17$ and $\Sigma 99$ <110> grain boundary structures closely approximating the 90° misorientation are currently underway.

ACKNOWLEDGEMENT

We thank Dr. I. Yamada for providing the ICB Al samples. This work is supported by the Director, Office of Energy Research, Office of Basic Energy Sciences, Materials Sciences Division of the U.S. Department of Energy under contract No.DE-AC03-76SF00098.

FIGURE CAPTIONS

Fig. 1 High resolution images of microstructures of porous oxides produced by thermal decomposition of $Mg(OH)_2$ (a) and $Al(OH)_3$ (b).

Fig. 2 Low magnification view of θ' precipitates in Al-4%Cu alloy (imaged in a 101 θ' reflection) illustrating precipitates with faceted morphology, produced by low temperature aging, necessary for high resolution microscopy of precipitate edges.

Fig. 3 High resolution micrograph of the edge of a faceted θ' plate in Al-4% Cu. Extra half plane in the matrix terminating at the top left corner of the plate is marked by arrow.

Fig.4 Atomic structure at the end of a γ' precipitate plate in Al-Ag alloy with Burgers circuit illustrating the presence of self-accommodating stack of Shockley partial dislocations that produces the required structural change from the fcc matrix to the hcp precipitate structure (courtesy Phil. Mag.).

Fig. 5 Silicon precipitate in Al-Si alloy showing both cube-cube and cube-twin orientation relationship(a). The particle is a triangular plate seen on edge and along one of its straight faces (left). Image simulations of two alternative models of unrelaxed interface are shown in (b) and (c).

Fig. 6 Cross sectional view of heteroepitaxial Al-Si interface produced by ICB deposition of Al on {111} Si (a) and two alternative image simulations of the same interface(b) and (c) based on one (b) and three (c) Si bonds coupled to Al [18].

Fig.7 Low magnification view of continuous bicrystal structure of Al grown on {100} Si showing curved boundaries in unannealed sample (a) and faceted boundaries in annealed sample (b).

Fig. 8 High resolution image of typical facet on Al 90° <110> grain boundary in symmetrical orientation.

Fig. 9 High resolution image of typical facet on Al 90° <110> grain boundary in asymmetrical orientation.

REFERENCES

1. J.W. Cahn and G. Kalonji, Proc. Int. Conf. Solid-Solid Phase Transformations, H.I. Aaronson, D.E. Laughlin, R.F Sekerka and C.M. Wayman, eds., The Metallurgical Society of AIME, (1982)
2. H.F. Fischmeister, J. de Physique, 46, Coll. C4-3 (1985)
3. W. Mader, G. Necker, S. Babcock and R.W. Balluffi, Scr. Met. 21, 555 (1987)
4. D.J. Eaglesham, C.J. Kiely, D. Cherns and M. Missous, Phil. Mag., in press
5. U. Dahmen, Acta Met. 30, 63 (1982)
6. J.D. Bernal and A.L. Mackey, Tschermaks min. u. petr. Mitt. 10,331 (1965)
7. J. Green, J. Mater. Sci. 18, 637 (1983)
8. A.F. Moodie and C.J. Warble, J. Cryst. Growth 74, 89 (1986)
9. M.G. Kim, U. Dahmen and A.W. Searcy, J. Am. Ceram. Soc. 70, 146 (1987)
10. U. Dahmen, M.G. Kim and A.W. Searcy, Ultramicroscopy 23, 365 (1987)
11. A. Zangwill, Physics at Surfaces, Cambridge Univ. Press, N.Y. (1988)
12. U. Dahmen and K.H. Westmacott, Scripta Met. 17, 1241, (1983)
13. J. Howe, U. Dahmen and R. Gronsky, Phil. Mag. A 56, 31 (1987)
14. A. Saulnier, Mem, Sci. Rev. Metallurg. 58, 615 (1961)
15. K.H. Westmacott and U. Dahmen, Proc. EMSA (1982), p. 620, G.W. Bailey, ed.
16. K.H. Westmacott and U. Dahmen, Proc. Int. Conf. Phase Transf., Cambridge, (1987), in press
17. H.I. Aaronson, in Decomposition of Austenite by Diffusional Processes, Intercience Publ., New York, 387
18. F. LeGoues, W. Krakow and P.S. Ho, Phil. Mag. A 53, 833, (1986)
19. I. Yamada, H. Inokawa and T. Takagi, J. Appl. Phys. 56, 2746 (1984)
20. U. Dahmen and K.H. Westmacott, Scr. Met. 22, 1678 (1988)
21. M.C. Madden and B.M. Tracy, Proc. EMSA (1987), p. 362, G.W. Bailey, ed.

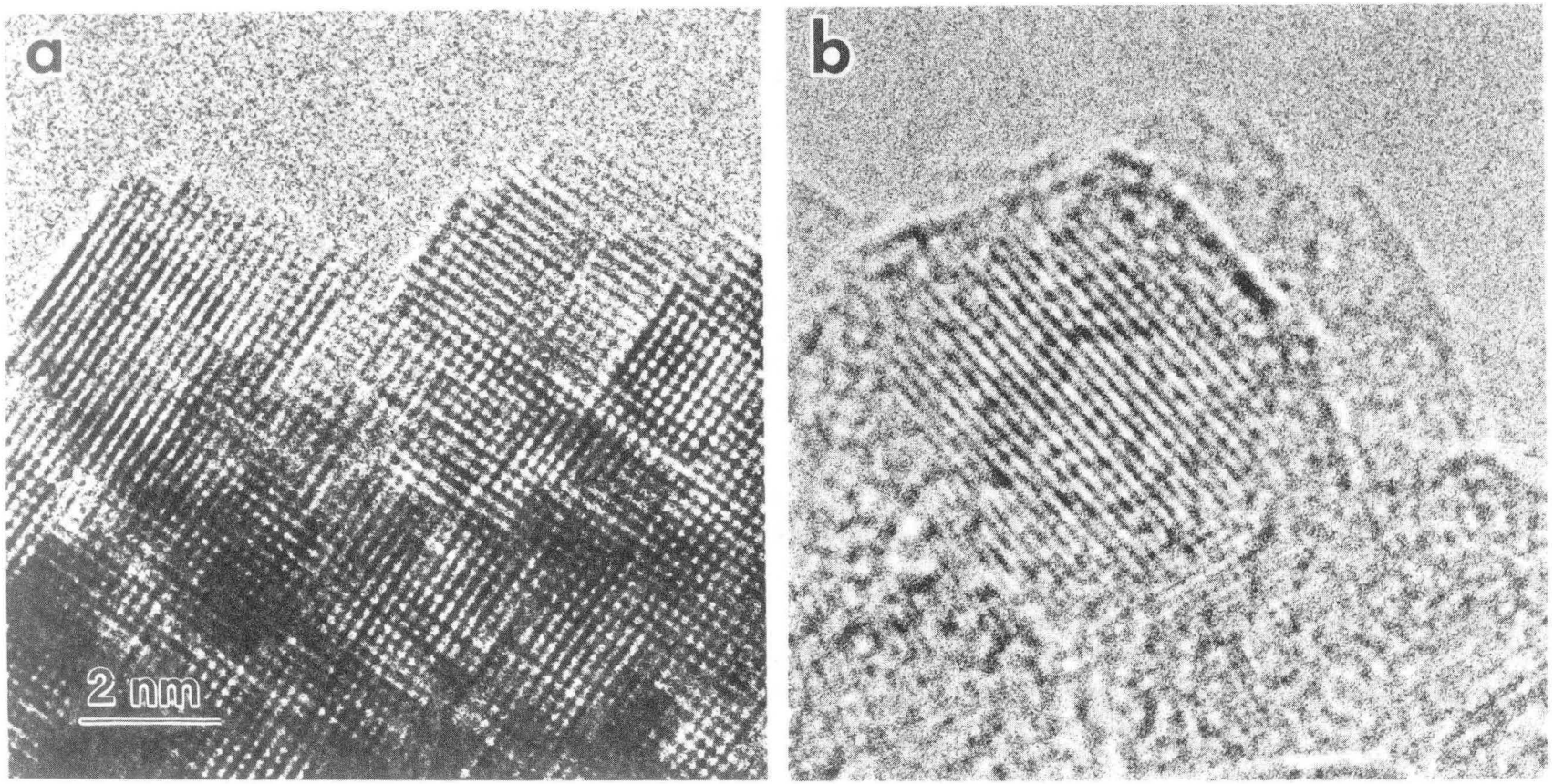

XBB 892-1096

FIGURE 1

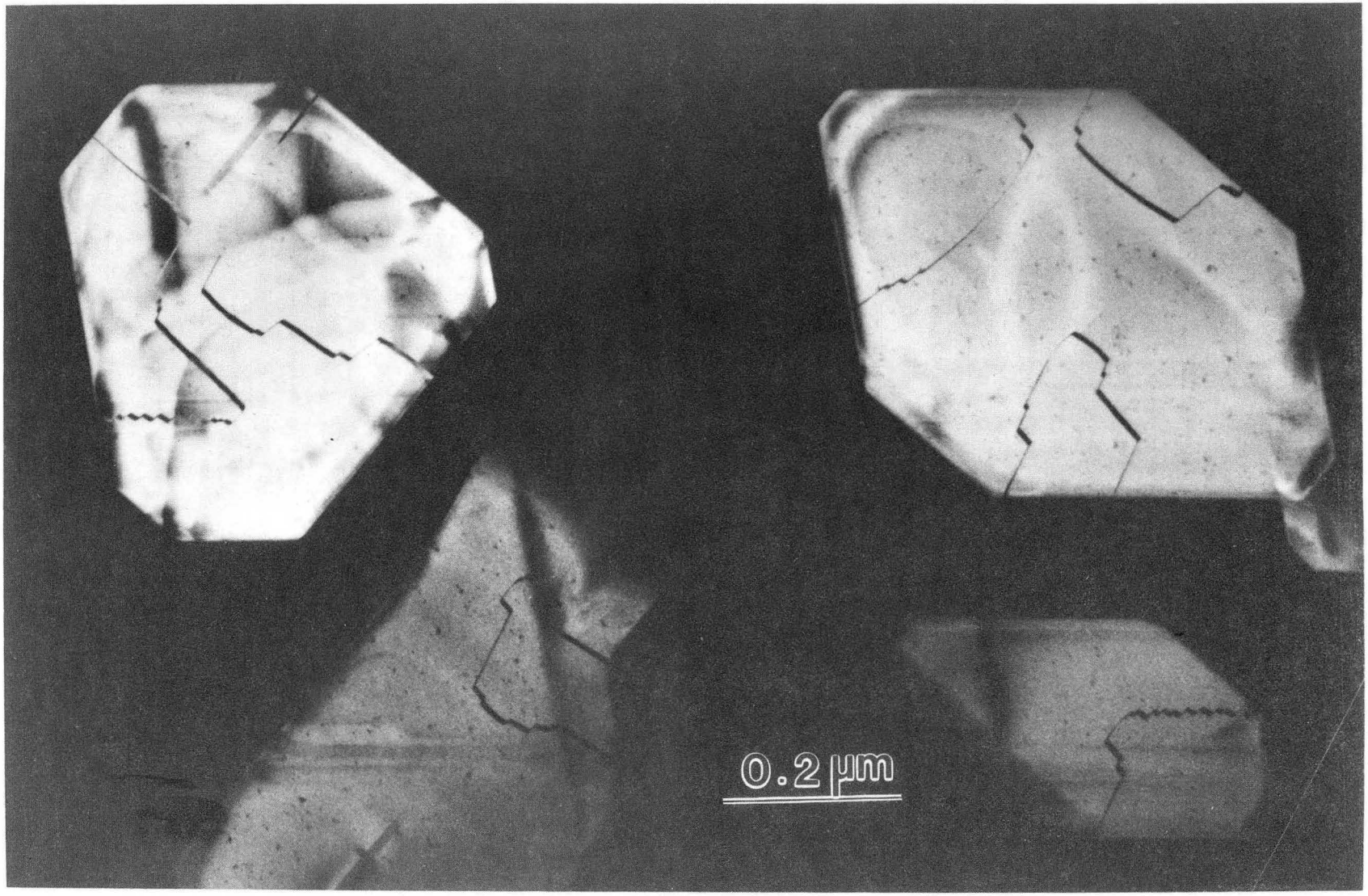

XBB 892-1098

FIGURE 2

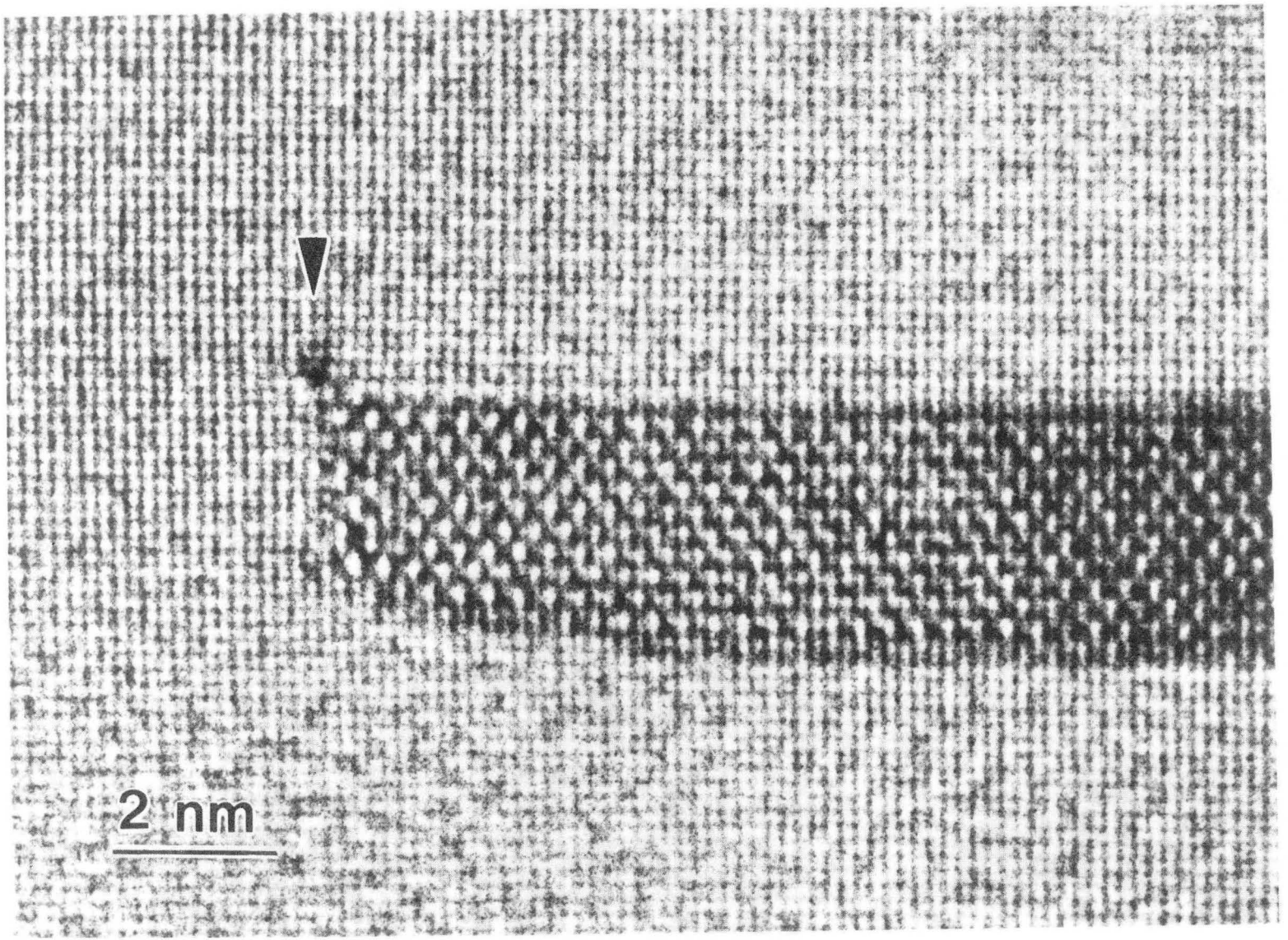

XBB 892-1097

FIGURE 3

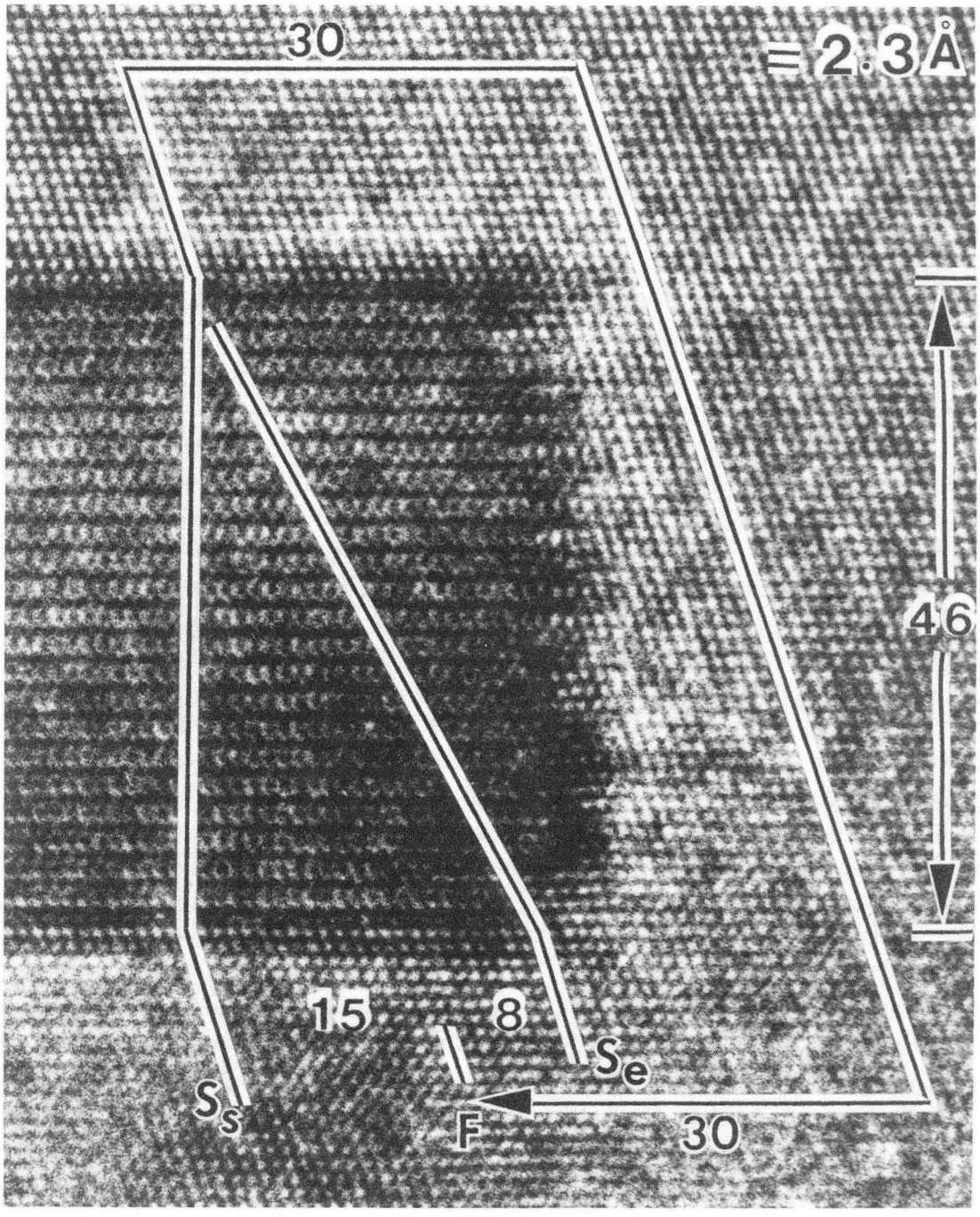

XBB 840-9360

FIGURE 4

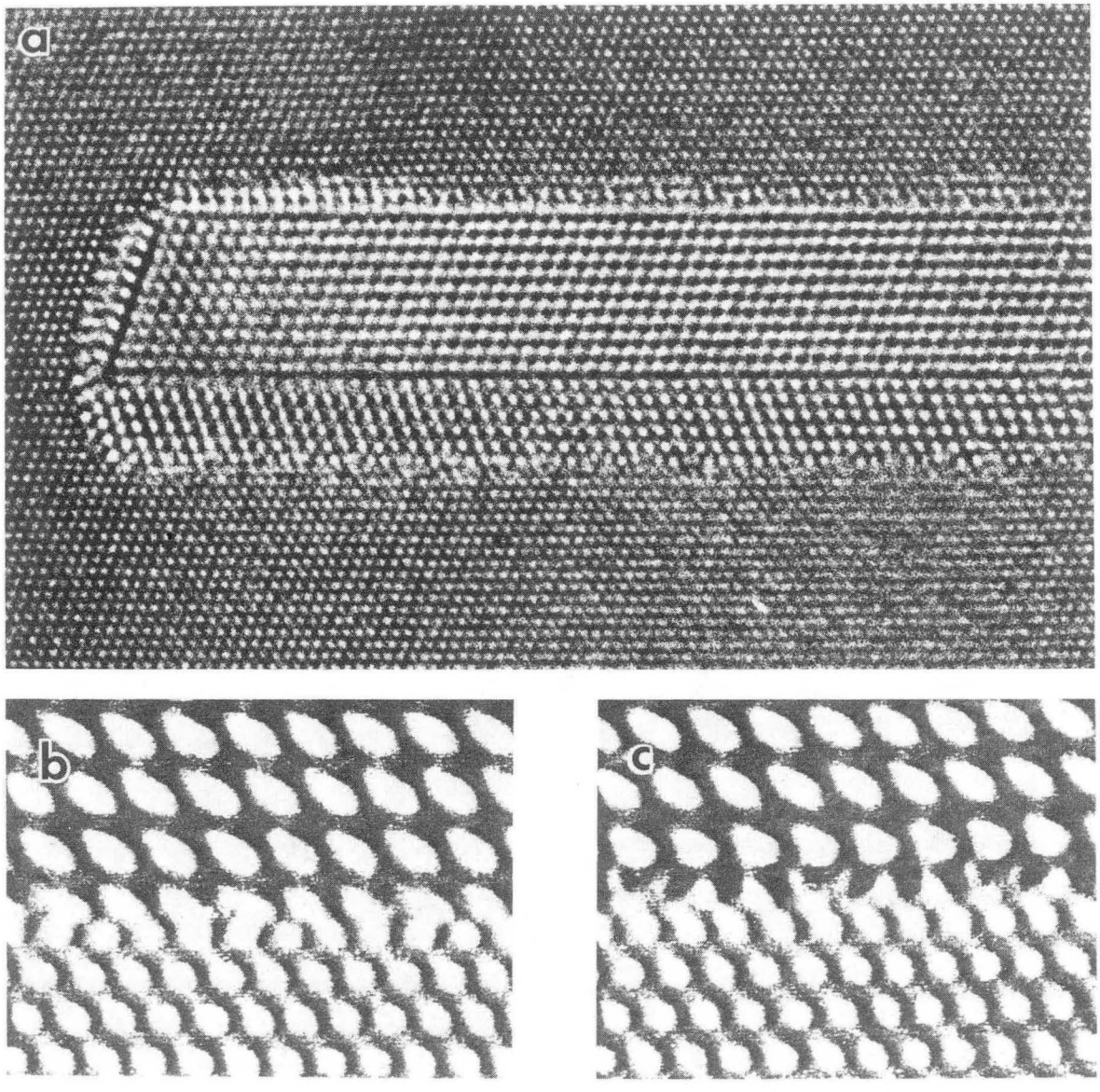

XBB 892-1099

FIGURE 5

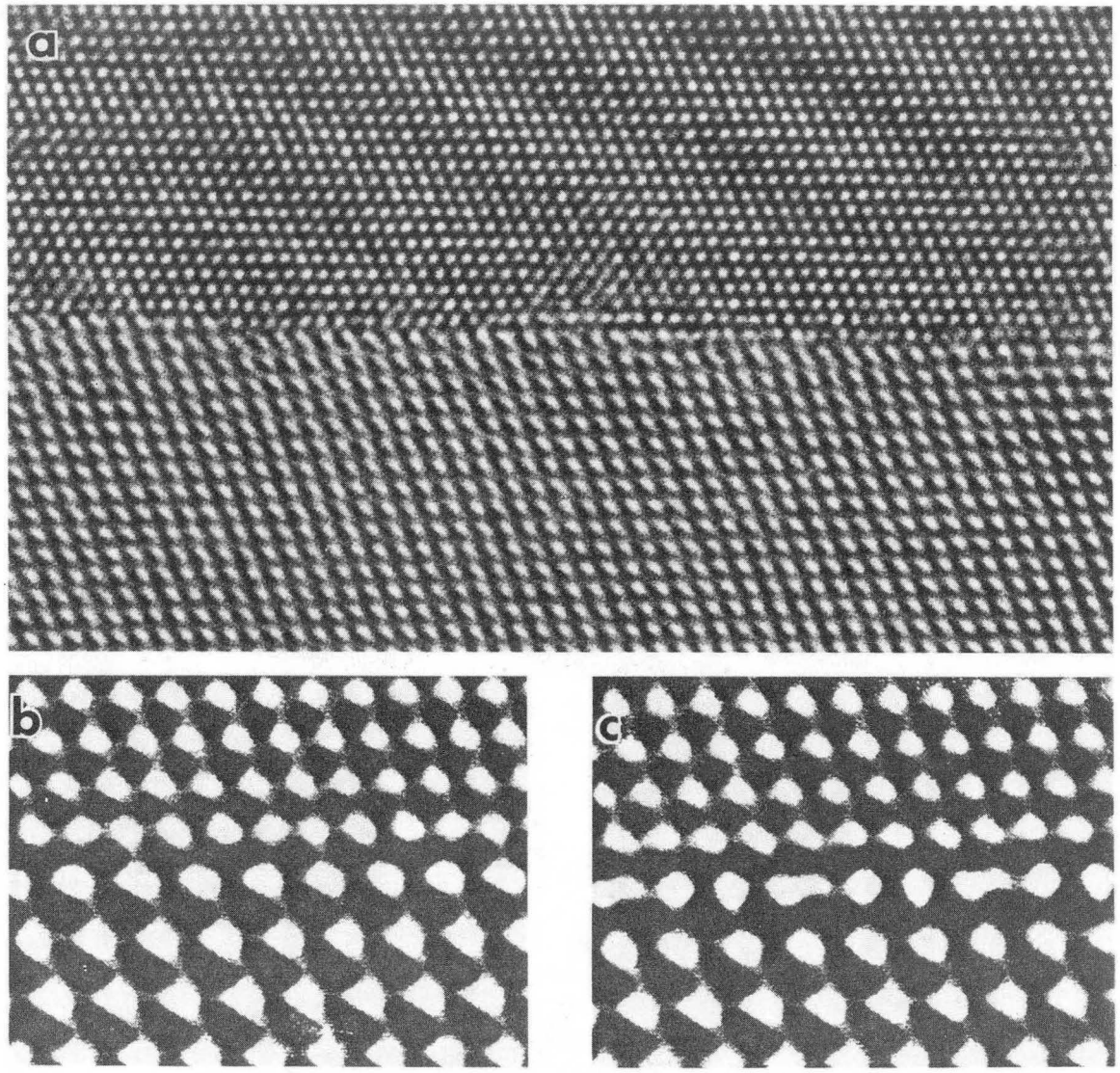

XBB 892-1100

FIGURE 6

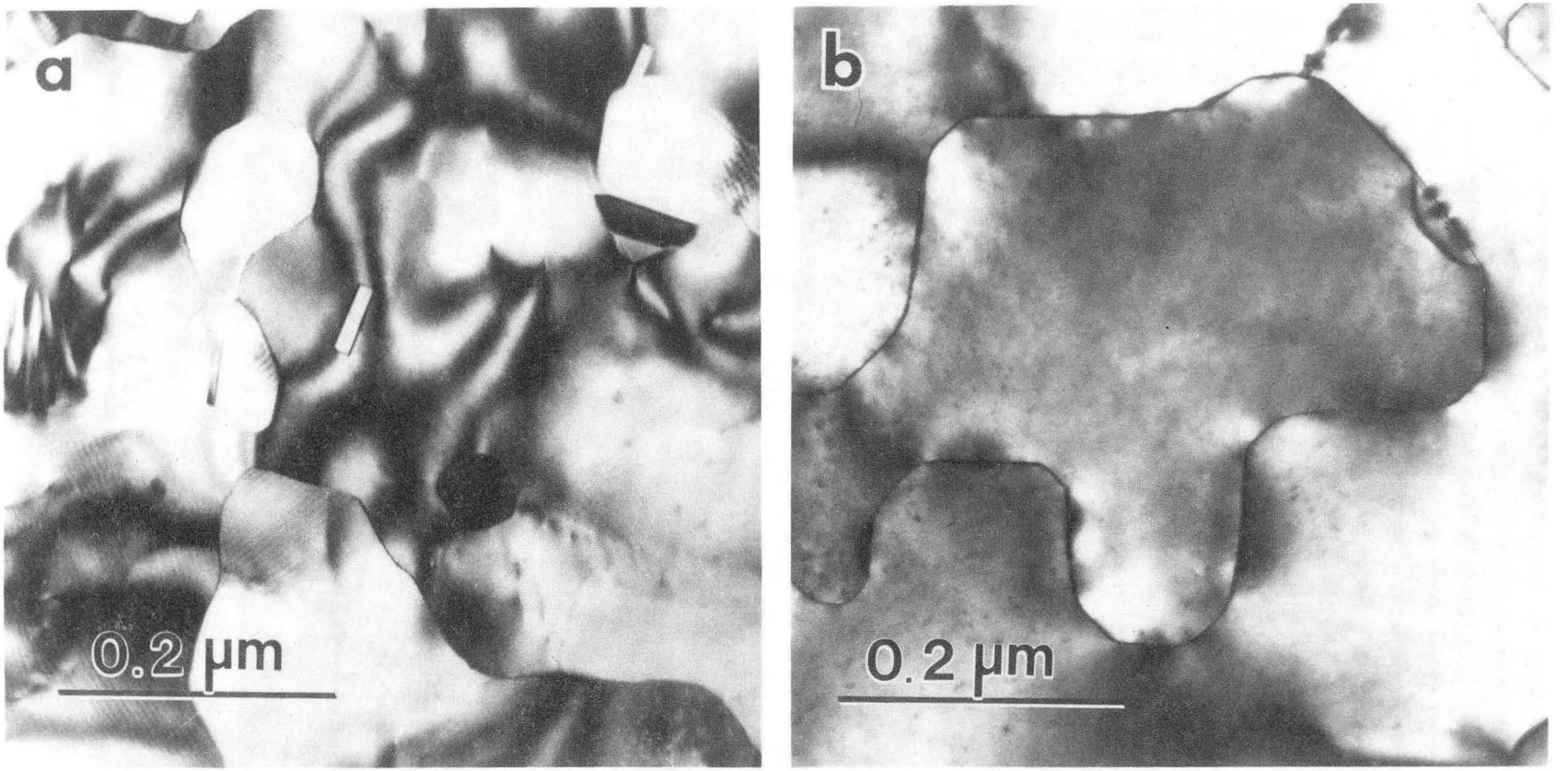

FIGURE 7

XBB 892-1101

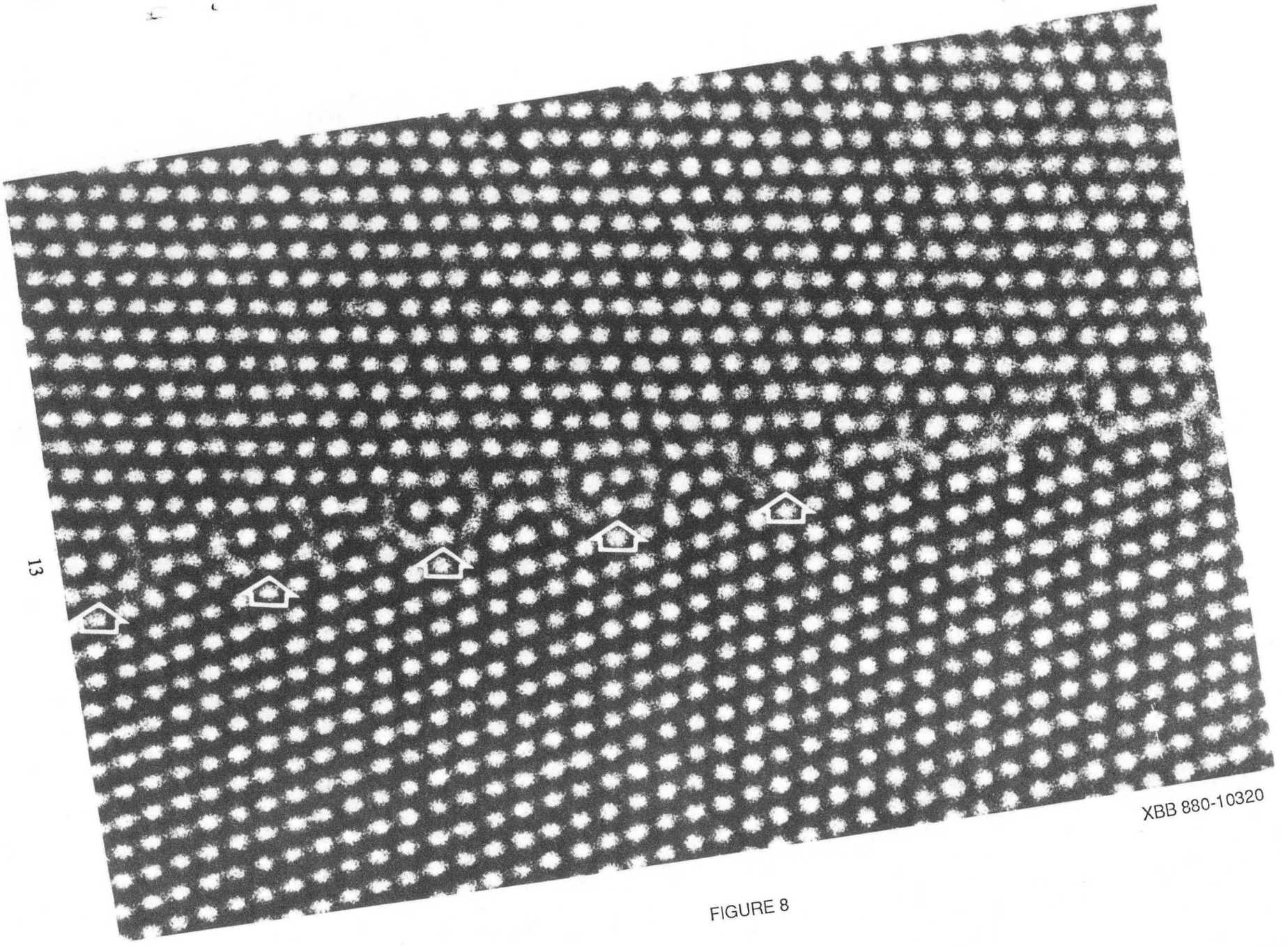

XBB 880-10320

FIGURE 8

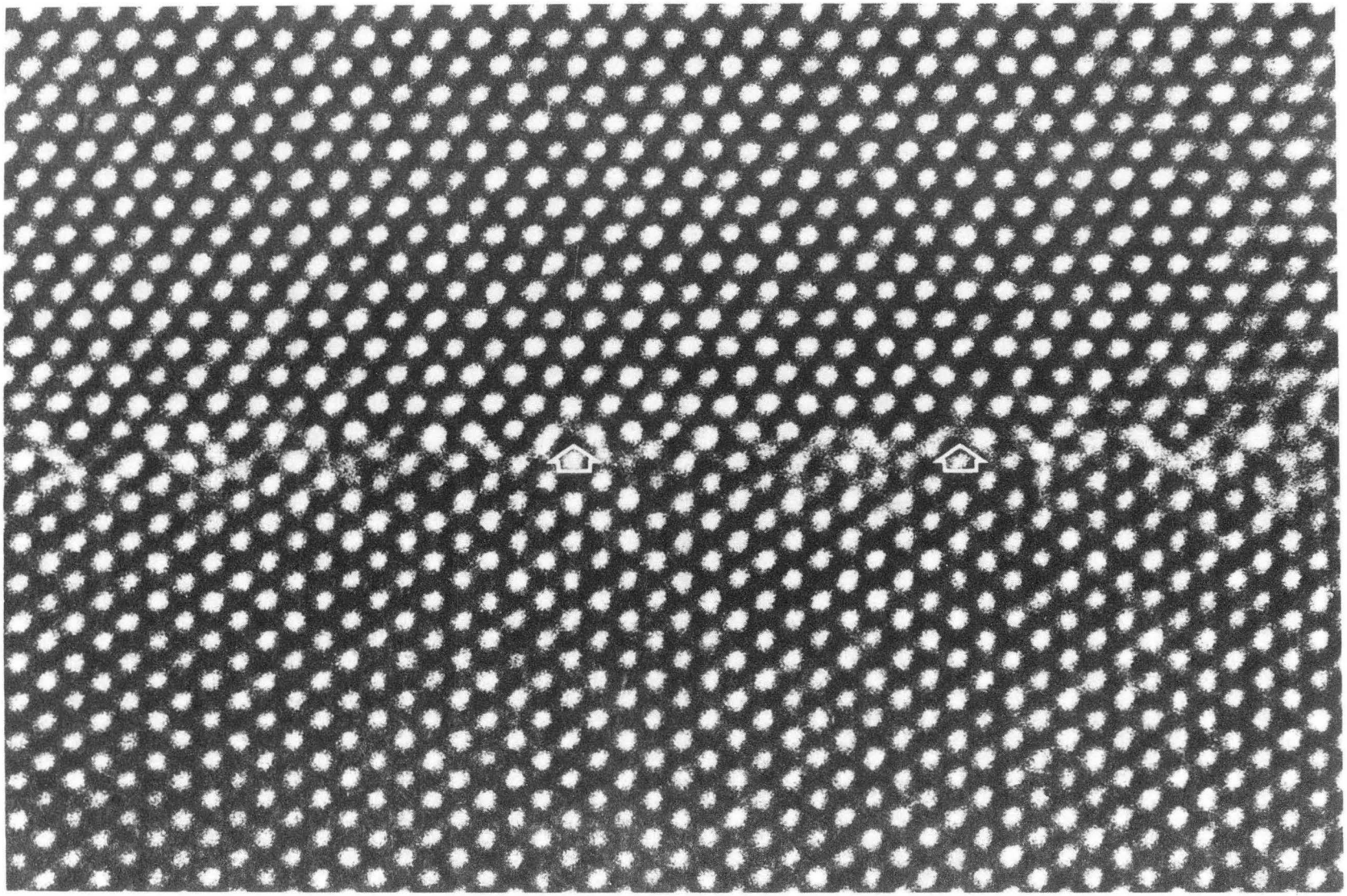

XBB 880-10319

FIGURE 9

LAWRENCE BERKELEY LABORATORY
TECHNICAL INFORMATION DEPARTMENT
1 CYCLOTRON ROAD
BERKELEY, CALIFORNIA 94720